CEA Comité Español de Automática
XLVI JORNADAS AUTOMÁTICA CARTAGENA 2025
UNIVERSIDADE DA CORUÑA

Jornadas de Automática

Design of High-Load Actuators Based on Shape Memory Alloys

González, Jaime*, Martínez, Santiago, Copaci, Dorin

Dpto. de Ingeniería de Sistemas y Automática, Universidad Carlos III de Madrid, Avda. de la Universidad, 30, 28911, Leganés, España

To cite this article: González, J, Martínez , S, Copaci, D. 2025. Design of High-Load Actuators Based on Shape Memory Alloys. Jornadas de Automática, 46. https://doi.org/10.17979/ja-cea.2025.46.12242

Abstract

Shape Memory Alloys (SMAs) possess strong potential for integration as actuators in robotic applications due to their high power-to-weight ratio and ability to recover their original shape after deformation. Among their various forms, SMA wires and springs are the most commonly available on the market. In this context, this work presents the design of a test bench and an actuator based on SMA wires, aimed at displacing high loads in compact environments. The study includes the mechanical and electrical characterization of Nitinol wires with diameters of 1–2 mm under different loading conditions, the iterative development of five actuator prototypes, and an evaluation through finite element analysis and experimental testing. The final actuator architecture confirms the feasibility of SMA-based systems for high-load applications up to 6000 N, offering an alternative to conventional solutions based on electric motors.

Keywords: Shape Memory Alloys, Actuator Design, Robotics, Smart Materials, Mechanical Design, Mechatronic Systems, Intelligent Actuators, Finite Element Methods

Diseño de actuadores de alta carga basados en aleaciones con memoria de forma

Resumen

Las aleaciones con memoria de forma (SMA, por sus siglas en inglés) presentan un gran potencial para su integración como actuadores en aplicaciones robóticas, debido a su elevada relación potencia-peso y su capacidad de recuperar la forma original tras una deformación. Entre sus diferentes formas, los hilos y muelles de SMA son los formatos comúnmente disponibles en el mercado. En este contexto, se presenta el diseño de un banco de pruebas y de un actuador basado en hilos de SMA, orientado al desplazamiento de altas cargas en entornos compactos. El trabajo incluye la caracterización mecánica y eléctrica de fibras de Nitinol con diámetros de 1-2 mm bajo distintas condiciones de carga, el desarrollo iterativo de cinco prototipos de actuador y una evaluación mediante análisis por elementos finitos y ensayos experimentales. La arquitectura final del actuador confirma la viabilidad de sistemas basados en SMA para aplicaciones de alta carga de hasta 6000 N, como alternativa a soluciones convencionales con motores eléctricos.

Palabras clave: Aleaciones con Memoria de Forma, Diseño de Actuadores, Robótica, Materiales Inteligentes, Diseño Mecánico, Sistemas Mecatrónicos, Actuadores Inteligentes, Métodos de Elementos Finitos

1. Introducción

Shape Memory Alloys (SMAs) are metalic materials that can be deformed and return to their original shape after an increase of temperature. SMA materials, such as Nitinol, exhibit unique properties including the Shape Memory Effect and Superelasticity. These properties enable controlled mechanical deformation and recovery through temperature-induced phase transformations, offering a high power-to-weight ratio, silent operation, and simplified structure. While these materials have already been successfully integrated into robotic

*J. Gonzalez: jgmenoca@ing.uc3m.es

systems for precision mechanisms and low-load applications, their use in heavy-load scenarios remains limited and insufficiently studied.

This work presents the design, construction, and evaluation of a SMA-based actuator, capable of displacing heavy objects, along with the development of a novel test bench designed to test and characterize this actuator. The objective of the project is to explore the feasibility of implementing SMA-based actuators in scenarios that demand high force generation and compact design, with potential application in robotics and industrial environments. This study builds upon previous research conducted at the RoboticsLab of Universidad Carlos III de Madrid, aiming to extend the operational limits of SMA actuators. By combining electrical and mechanical characterization, finite element analysis (FEA), and iterative prototyping, this work proposes a compact actuator architecture optimized for both performance and structural integrity. A key contribution is the development of specialized testing platforms and control systems to evaluate the response of SMA wires and actuators under increasingly demanding load conditions.

1.1. Background

SMAs are metallic materials that can undergo significant deformation and recover their original shape when subjected to temperature changes. This behavior is primarily attributed to the reversible transformation between their two stable crystalline phases: martensite and austenite. These two crystalline structures are stable at different ranges of temperature, meaning that the material adopts the martensite structure at lower temperatures and the austenite structure at higher temperatures (Reynolds, 2003). These materials exhibit two key properties: Shape Memory Effect (SME) and Superelasticity (SE). SME is caused by a rise in temperature that triggers a transition from martensite to austenite, allowing the material to recover its original shape, while cooling reverses the process. SE, on the other hand, occurs in the austenite phase under constant temperature when stress induces a martensitic transformation, which reverts upon stress removal (Mohd Jani et al., 2014)(Ozbulut and Hurlebaus, 2011). These two properties have led to the integration of SMA actuators in a variety of fields such as aerospace (Hollenbach et al., 2006), biomedical devices (Pfeifer et al., 2013), and robotics (Deng and Tadesse, 2021)(Var and Jovanova, 2023).

Among the different SMA compositions, Nitinol (Nickel-Titanium alloy) stands out due to its high recoverable strain, good fatigue resistance, and biocompatibility (Mohammadgholipour and Billah, 2023). These characteristics make it especially interesting for actuator design, where compactness, efficiency, and silent operation are required. Despite extensive research and applications in lower load contexts and SMA wires with low diameters, the use of SMA wires in systems designed for lifting heavy loads remains relatively underexplored. In robotic actuation, SMAs have been used to create grippers, artificial muscles, and bio-inspired mechanisms. However, these implementations typically focus on precision rather than force. To address this gap, the present work investigates the mechanical behavior of SMA wires under high-load conditions and proposes an actuator architecture that optimizes both structural reliability and force generation.

2. Materials and Methods

This section presents the components, materials, and tools used for this project, as well as the actuator's design evolution and its control strategy.

2.1. SMA Wire Characterization

The first stage of this work involved the characterization of SMA wires to determine their suitability for high-load actuation applications. Given the objective of designing a compact actuator capable of displacing heavy objects, it was essential to first quantify the mechanical and electrical behavior of the SMA wires under controlled conditions.

Two wire diameters were chosen for evaluation: 1 mm and 2 mm, significantly larger than the more common sub-millimeter SMA wires used in biomedical or robotics applications. The choice of these diameters was motivated by the need to generate higher contraction forces while maintaining compatibility with compact actuator geometries. Manufacturer data was limited to diameters below 0.5 mm, so theoretical calculations and experimental validation were required to estimate performance metrics such as activation temperature, electrical resistance, maximum current, and rated load for the selected wire sizes, which can be seen in Table 1.

Table 1: Parameters of interest of SMA wires.

	Wire 1	Wire 2
Diameter [mm]	1	2
Activation temperature [ºC]	40	40
Resistance [Ω]	1.08	0.27
Current [A]	16	64
Theoretical rated load [N]	400	1200

To conduct the characterization, a dedicated experimental workbench was used, developed for previous experiments at RoboticsLab (Copaci et al., 2024) and displayed in Figure 1. The structure consists of an aluminum frame with an upper fixed platform and a lower movable platform. The SMA wire is fixed between both platforms, allowing vertical contraction to be measured. The following sensors and components were integrated into the bench to enable closed-loop measurements: A position magnetic sensor, coupled with a linear magnetic strip, which provides incremental displacement readings, a Hall-effect current sensor that measures the current passing through the wire during actuation, a cooling ventilator system, and springs to simulate heavy loads. The specifications of these springs can be found in Table 2.

Table 2: Spring specifications.

	Light	Medium
Stiffness K [N/m]	94	185
External diameter [mm]	32	32
Internal diameter [mm]	16	16
Wire width [mm]	6.8	6.8
Wire height [mm]	3.3	4.0
Length [mm]	38	38

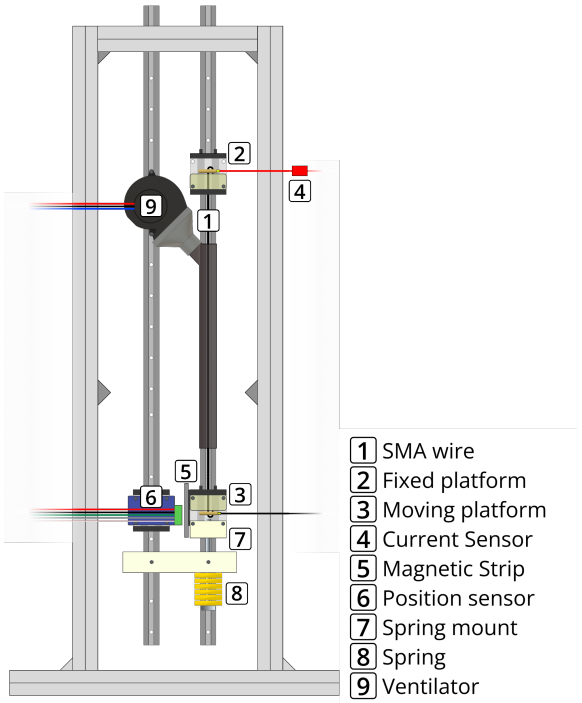

Figure 1: Wire characterization workbench.

To ensure precise and repeatable characterization of SMA wires under load, a closed-loop control system was implemented using a dedicated experimental platform. The system integrates both control electronics and data acquisition tools, enabling dynamic regulation of wire contraction and real-time monitoring of performance parameters. The control architecture is centered around an STM32F4 microcontroller, which orchestrates signal generation, sensor feedback, and communication with the host interface. Actuation is achieved by direct resistive heating of the SMA wires via a PWM signal, with duty cycle modulation based on displacement error. Power regulation is managed by a custom electronics board equipped with MOSFET transistors, capable of handling currents up to 20 A. Current is monitored using a Hall-effect sensor, while wire displacement is measured through a magnetic position sensor, which tracks 2 mm increments along a coded strip.

The control loop is implemented in Simulink and deployed to the microcontroller. Two Simulink modules are used: one for configuring control parameters and generating embedded code, and another for real-time visualization and interaction. The host interface allows users to input target displacements, monitor current and position, and toggle between manual and automated operation modes. A bilinear PID (BPID) controller was selected for wire actuation. This strategy combines a conventional PID with a bilinear compensator to enable discrete-time control of the nonlinear SMA system. Due to the wire's integrative behavior the integral gain was set to zero in all cases to avoid error accumulation. Control parameters were tuned empirically for each wire diameter, ensuring fast response with minimal overshoot.

A total of 40 configurations were tested across the two wire diameters and spring types. Each trial began by fixing a wire of known length and diameter between the platforms and selecting an appropriate spring to generate resistive force. A reference displacement value was set, and the current was gradually increased via PWM-controlled actuation until the desired contraction was achieved. This reference value was augmented until failure. During this process, sensor data was recorded and processed in MATLAB. Maximum displacement and current were analyzed to evaluate control accuracy and characterize SMA behavior under specific loads. Key performance metrics such as experimental mean (μ_{exp}), Relative Error (RE), Mean Absolute Error (MAE), Root Mean Square Error (RMSE), and standard deviation (σ) were used to quantify repeatability and inform the actuator design process.

The outcomes of these tests were used to determine the number of wires and the actuator geometry needed to achieve the target lifting force of 6000 N under realistic operating conditions. The actuator geometry and design parameters are detailed in the next section.

2.2. Actuator Design and Prototyping

The actuator design process was guided by the objective of maximizing force output within a compact, modular structure suitable for integration into industrial systems. Given the relatively low strain and slow recovery of SMA wires, the design emphasized mechanical amplification and structural resilience. A series of five actuator prototypes were developed iteratively, each introducing modifications in geometry, materials, or wire configuration based on previous performance evaluations. All designs share a common architecture: two interlocking cylindrical bodies with concentric perforations to house the SMA wires. These perforations guide the wires along a path, allowing either a direct or looped configuration, and are secured laterally with fasteners. A central perforation accommodates a structural mounting screw for integration into the testing workbench. This geometry facilitates modular assembly while distributing load uniformly during contraction. In the following paragraphs, each of the iterations of the actuator prototypes are described, and their geometries are all included in Table 3 and pictured in Figure 2,

Table 3: Geometric and functional specifications of the actuator base.

	I	II	III	IV	V
Diameter [mm]	168	75	120	28	80
Height [mm]	20	10	40	12.5	30
Perforations for wires	20	20	5	10	10
Nitinol wires	10	10	5	5	5
Lateral fasteners [-]	20	20	20	10	10
Number of parts	1	1	2	2	2

- Prototypes I and II were fabricated in post-cured resin. These early designs featured 20 perforations with 10 looped wires, chosen to assess wire spacing, clamping reliability, and electrical isolation in polymer-based structures. Prototype II reduced overall dimensions to improve compactness, serving as a benchmark for size-performance tradeoffs.

- Prototype III had a design focused on structural stability. A lower steel plate was added to reduce deformation under load, and the number of wire paths was halved to

five, eliminating the looping configuration. Bronze fasteners were embedded to ensure electrical conduction without compromising mechanical fixation. This configuration preserved electrical insulation while improving force distribution and wire handling.

- Prototypes IV and V transitioned to full-steel designs, in favor of mechanical robustness. A new two-piece construction enabled easier wire installation without precise pre-bending, improving assembly repeatability. Prototype IV prioritized minimal footprint, while Prototype V increased diameter and spacing between wires to reduce bending stress, improve fatigue resistance, and facilitate high-load operation.

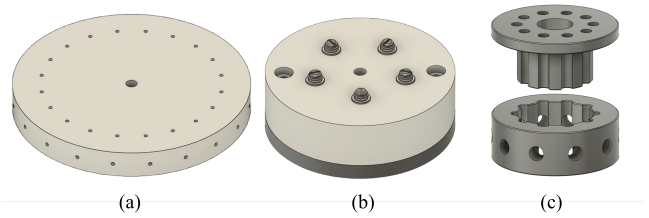

Figure 2: Prototype design evolution: Prototype I (a), Prototype III (b), and Prototype V (c).

2.3. Simulation and Testing

To evaluate the mechanical performance of the actuator prototypes under simulated and physical load conditions, a two-step validation strategy was proposed. Finite Element Analysis (FEA) simulations were conducted using Autodesk Inventor to predict structural behavior under idealized conditions, which would be followed by real-world testing using a custom-built actuator workbench. This combined approach allowed for the comparison of theoretical stress-strain responses against empirical performance metrics.

Prior to fabrication, each actuator prototype was fully modeled in Fusion 360 and then imported into Autodesk Inventor for simulation. FEA studies were conducted to assess stress distribution, deformation, and displacement under a range of applied loads corresponding to the maximum estimated forces from SMA wire contraction.

The simulation process consisted of several sequential steps. The actuator was virtually fixed at its central mounting point, while lateral constraints were introduced to replicate the clamping effect of the fasteners. In assemblies composed of two parts, contact definitions were included at the interface between the steel disks and the surrounding material. Tensile forces were applied at the wire perforations to simulate contraction, with equal and opposite loads used in looped configurations to maintain balanced loading conditions. Each component was assigned material properties derived from fabrication data, allowing the model to reflect variations in elasticity and yield strength across different prototypes. A parametric sweep was conducted by simulating five distinct load cases, increasing in 20% increments from the baseline up to the theoretical maximum load. This resulted in a total of 25 simulation studies covering all prototype variants.

Key performance metrics evaluated in the simulations included:

- Safety Factor (SF), defined as the ratio between the material's yield strength and the maximum equivalent stress. It is expressed as $\mathrm{SF} = \sigma_{\text{yield}}/\sigma_{\text{von Mises}}$.
- Von Mises Stress, used as a scalar measure to predict yielding of ductile materials.
- Total Displacement, computed as the Euclidean norm of displacements in the three spatial directions
- Elastic Deformation, related to the strain energy stored in the material under load.
- Contact Force and Pressure Distributions, extracted from interface interactions for multi-part prototypes.

A second custom workbench was developed to physically evaluate the actuator prototypes under realistic loading conditions. The structure was built around a three-dimensional aluminum frame capable of housing up to three actuators simultaneously. The layout incorporates an antagonistic actuator for recovery and a brake-lever system to simulate load through torque resistance. The main components include an electromagnetic particle brake, capable of delivering up to 200 Nm of torque, a static torque sensor, based on strain gauge technology, and a power supply regulator to energize the brake. This second workbench is pictured in Figure 3.

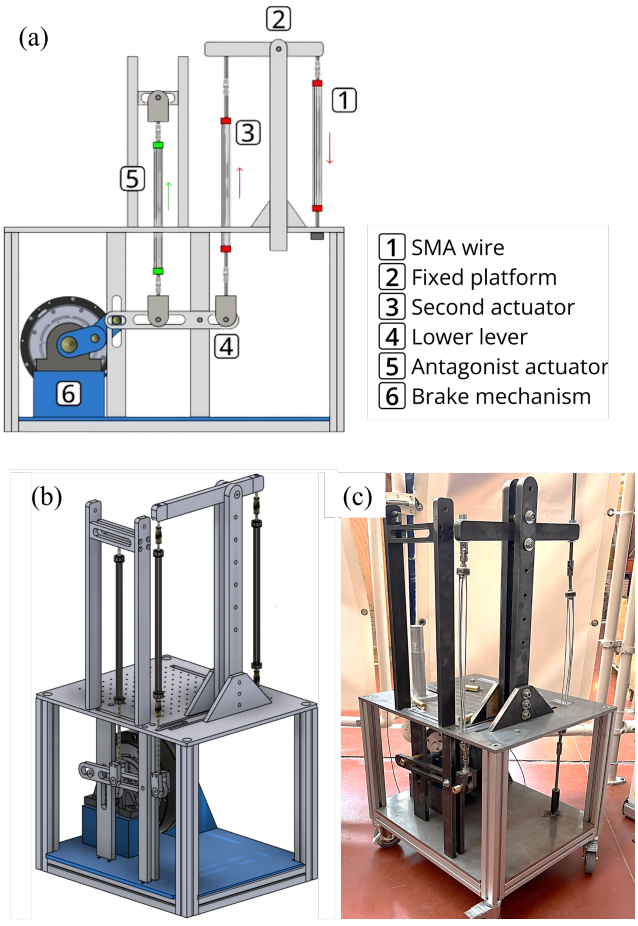

Figure 3: Actuator evaluation workbench: Components diagram (a), 3D-model (b) and finished workbench (c).

Each actuator is connected through a mechanical lever system that transmits force to the brake. The generated torque is measured and converted into equivalent force using the torque equation $\tau = F \cdot r$, where the radius corresponds to the lever arm length. This allows the emulation of variable weights without physical mass addition, improving repeatability and safety.

The test procedure follows a similar control methodology to the one used for wire characterization. Activation is achieved by direct heating via PWM-controlled current. Control is centralized through the STM32F4 microcontroller, with real-time monitoring and parameter adjustment enabled via a Simulink-based interface. Two Simulink files structure the control flow: one deploys the controller to the microcontroller, and the other enables the user to set reference values and visualize sensor data. During testing, variations in torque readings before and after actuation are captured and processed to determine the effective lifting force.

Although the physical experiments were not executed due to component availability, the complete testing framework was designed and validated in simulation. This system offers a controlled environment for future actuator validation, ensuring accurate, repeatable load testing and data acquisition for future iterations.

3. Results

This section presents the results obtained during the characterization and testing phases, both at the wire level and at the actuator level. The analysis includes experimental measurements from wire contraction and simulation data from FEA.

3.1. Wire Characterization Results

A total of 40 trials were carried out, combining two SMA wire diameters and two spring stiffness levels. Displacement data was collected using the magnetic position sensor, and the force was inferred through Hooke's Law based on the measured spring deformation. The results can be seen in Table 4.

Across all tests, the 1 mm wire demonstrated more consistent actuation behavior, while the 2 mm wire exhibited higher forces but introduced greater variability due to increased thermal inertia. The experimental results validated the estimated rated loads. These findings informed the final selection of wire configurations for actuator integration.

3.2. Actuator Evaluation

FEA results highlighted the impact of geometry and material choice on structural behavior. The results of these studies are found in Table 5. Key findings include:

- Safety Factor: Versions I and II (polymer-based) showed safety factors lesser than 1.5 under maximum theoretical loads, while Versions IV and V (full-steel) consistently exceeded a safety factor of 3, meeting industrial reliability thresholds.
- Von Mises Stress: Stress concentrations were highest at the wire perforations and screw interfaces. The bronze fasteners in Prototype III helped distribute these loads more effectively.
- Displacement and Deformation: All prototypes maintained deformation within acceptable limits. Version V exhibited minimal displacement ($< 0.2\,\text{mm}$) at maximum load, confirming its rigidity.
- Contact Forces and Pressures: Excessive contact pressure was observed in early prototypes with narrow perforation spacing. Adjustments in Prototype V reduced localized stress peaks, improving fatigue resistance.

Prototype V, the final and most robust design, demonstrated the best mechanical performance under simulated high-load conditions.

Although complete actuator trials were delayed due to unavailability of mechanical parts, preliminary testing confirmed the viability of the torque-brake-based evaluation methodology. Simulated torque loads matched expected force outputs from the SMA wire bundles, and the electronics platform was validated for synchronous control and data acquisition. The experimental setup is ready for future trials and will enable full quantification of lifting capacity, thermal cycling behavior, and actuator lifespan under industrial load profiles.

4. Discussion

This section presents a critical analysis of the performance of the SMA wires and the actuator prototypes, based on both experimental wire characterization and simulation results. The discussion focuses on the reliability, limitations, and practical implications of the proposed actuator system.

The experimental results confirmed that Nitinol wires of 1 mm and 2 mm diameter can be used effectively in high-load actuation scenarios. The 1 mm wire displayed more predictable and repeatable behavior, with lower power consumption and shorter recovery times. In contrast, the 2 mm wire offered significantly higher force output but introduced challenges related to heat dissipation and activation current thresholds. The bilinear PID controller implemented in the test platform successfully regulated wire contraction with low steady-state error, especially in the 1 mm configurations. However, actuation repeatability was affected by environmental factors such as ambient temperature and cooling efficiency, particularly in longer cycle operations.

Table 4: Experimental results with different springs and forces.

Configuration	$F_{\max}$ [N]	Spring	Exp. [mm]	μ_{exp} [mm]	RE [%]	MAE [mm]	RMSE [mm]	σ [mm]
∅1 – Light	400	Light	4.26	4.081	4.20	0.178	0.241	0.199
∅1 – Medium	400	Medium	2.16	1.938	10.28	0.232	0.278	0.148
∅2 – Light	1200	Light	12.77	10.709	16.16	1.905	2.076	0.390
∅2 – Medium	1200	Medium	6.49	5.824	10.26	0.661	0.795	0.605

Table 5: FEA simulation results for different actuator prototypes and applied loads.

Configuration	Safety factor	Von Mises Stress [MPa]	Displacement [mm]	Deformation [%]	Contact force [N]	Contact pressure [MPa]
V – 1200 N	15.000	7.367	5.00e-05	4.56e-05	4.563	4.637
V – 2400 N	14.048	14.735	1.00e-04	9.12e-05	9.127	9.274
V – 3600 N	9.365	22.103	1.50e-04	1.37e-04	13.690	13.911
V – 4800 N	7.024	29.470	2.00e-04	1.82e-04	18.253	18.549
V – 6000 N	5.619	36.838	2.50e-04	2.28e-04	22.817	23.186
IV – 1200 N	11.749	17.618	1.08e-04	1.44e-04	4.230	13.198
IV – 2400 N	5.875	35.237	2.17e-04	2.88e-04	8.459	26.396
IV – 3600 N	3.916	52.855	3.25e-04	4.32e-04	12.689	39.594
IV – 4800 N	2.937	70.474	4.33e-04	5.76e-04	16.919	52.792
IV – 6000 N	2.350	88.000	5.42e-04	7.21e-04	21.148	65.990
III – 1200 N	5.051	3.959	8.00e-03	3.00e-03	9.025	0.850
III – 2400 N	2.526	7.919	1.60e-02	5.00e-03	18.050	1.700
III – 3600 N	1.684	11.878	2.50e-02	8.00e-03	27.076	2.551
III – 4800 N	1.263	15.838	3.30e-02	1.00e-02	36.101	3.401
III – 6000 N	1.010	19.797	4.10e-02	1.30e-02	45.126	4.251
II – 1200 N	2.537	7.882	1.00e-02	2.00e-03	–	–
II – 2400 N	1.269	15.764	1.90e-02	4.00e-03	–	–
II – 3600 N	0.846	23.646	2.90e-02	6.00e-03	–	–
II – 4800 N	0.634	31.528	3.90e-02	8.00e-03	–	–
II – 6000 N	0.507	39.410	4.80e-02	9.00e-03	–	–
I – 1200 N	7.764	2.576	4.00e-03	2.00e-03	–	–
I – 2400 N	3.882	5.152	9.00e-03	4.00e-03	–	–
I – 3600 N	2.588	7.728	1.30e-02	6.00e-03	–	–
I – 4800 N	1.941	10.304	1.80e-02	8.00e-03	–	–
I – 6000 N	1.553	12.880	2.20e-02	9.00e-03	–	–

The iterative design process resulted in five actuator prototypes, each incorporating structural and functional improvements based on prior evaluations. FEA validated that only the final designs exhibited safety factors above 3 under full-load conditions. Prototype V demonstrated superior performance in all simulated metrics, making it the most promising candidate for implementation.

The workbench was comprehensively designed and validated. Its torque-based load simulation offers a scalable platform for future experimental trials on endurance testing and dynamic load evaluation.

Overall, the methodology developed in this project successfully established a foundation for SMA-based high-load actuators. Future work will focus on full-scale physical testing, long-term fatigue assessment, and the integration of thermal management strategies to enable continuous operation.

Acknowledgements

This work is supported by the grant-funded project *ROBOSUB: "Robots inteligentes subterráneos para la transición ecológica y digital del subsuelo urbano"* (TED2021-129420B-I00), funded by MCIN/AEI/10.13039/501100011033 and the European Union's *"NextGeneration EU/PRTR"*; and by the R&D activity program with reference TEC-2024/TEC-62 and acronym iRoboCity2030-CM, granted by the Community of Madrid through the Directorate General for Research and Technological Innovation, under Order 5696/2024.

References

Copaci, D., Palenzuela, A. L., Moreno, L., Martínez, S., Balaguer, C., 2024. Characterization and control of shape memory alloy-based actuators for heavy payloads displacement. Results in Engineering 24, 103387. DOI: https://doi.org/10.1016/j.rineng.2024.103387

Deng, E., Tadesse, Y., Jan. 2021. A Soft 3D-Printed Robotic Hand Actuated by Coiled SMA. Actuators 10 (1), 6. DOI: 10.3390/act10010006

Hollenbach, U., Kapp, A., Stiller, C., 2006. Ferromagnetic shape memory microscanner system for automotive applications. International Journal of Applied Electromagnetics and Mechanics 23 (1-2), 107–112.

Mohammadgholipour, A., Billah, A. M., 2023. Mechanical properties and constitutive models of shape memory alloy for structural engineering: A review. Journal of Intelligent Material Systems and Structures 34 (20), 2335–2359. DOI: 10.1177/1045389X231185458

Mohd Jani, J., Leary, M., Subic, A., Gibson, M. A., Apr. 2014. A review of shape memory alloy research, applications and opportunities. Materials & Design (1980-2015) 56, 1078–1113. DOI: 10.1016/j.matdes.2013.11.084

Ozbulut, O., Hurlebaus, S., 11 2011. Seismic response control using shape memory alloys: A review. Journal of Intelligent Material Systems and Structures - J INTEL MAT SYST STRUCT 22, 1531–1549. DOI: 10.1177/1045389X11411220

Pfeifer, R., Müller, C. W., Hurschler, C., Kaierle, S., Wesling, V., Haferkamp, H., Jan. 2013. Adaptable Orthopedic Shape Memory Implants. Procedia CIRP 5, 253–258. DOI: 10.1016/j.procir.2013.01.050

Reynolds, D., 01 2003. A nonlinear thermodynamic model for phase transitions in shape memory alloy wires.

Var, S. C. S., Jovanova, J., Sep. 2023. Design of a Soft Underwater Gripper with SMA Actuation. Vol. ASME 2023 Conference on Smart Materials, Adaptive Structures and Intelligent Systems of Smart Materials, Adaptive Structures and Intelligent Systems. DOI: 10.1115/SMASIS2023-111702